ISPRS Annals of the Photogrammetry, Remote Sensing and Spatial Information Sciences, Volume XII-4/W2-2026
10th International Conference on Smart Data and Smart Cities (SDSC), 29 September–1 October 2026, Sofia, Bulgaria

Graph-Based Safe-Routing for Flood-Aware Evacuation in Urban Environments

Eduardo Manuel Verdugo Fernández, Al Maimun As Samee, Lukas Arzoumanidis, Huynh Duc An Son Nguyen, Youness Dehbi

Computational Methods Lab, HafenCity University, Hamburg, Germany -
{eduardo.fernandez, al.samee, lukas.arzoumanidis, son.nguyen, youness.dehbi}@hcu-hamburg.de

Keywords: flood risk, evacuation planning, graph-based model, urban network analysis, safe-routing.

Abstract

Flooding presents a major hazard to urban citizens, particularly during the initial phase of an event when evacuation decisions must be made under limited spatial information. Despite recent advances in hydrological modelling and early warning systems, these approaches often do not provide route-level information required for operational evacuation planning. This study presents a graph-based spatial framework for computing safe evacuation routes under flood conditions. The approach constructs a weighted graph from open geospatial data, integrating buildings, street network, and flood extent. Buildings are classified according to their extent of flood-exposure, while road segments intersecting flooded areas are assigned a prohibitively large cost and are therefore excluded from the routing process, whereas unaffected segments retain a finite cost proportional to their length. Safe routes are calculated using a shortest-path algorithm on the resulting flood-constrained weighted graph. The methodology is applied to a case study in Kremmen and Oranienburg, Germany, a flood-prone region in Brandenburg, demonstrating how inundation alters network connectivity and constrains evacuation options. The proposed framework supports the integration of semantic information and optimisation in evacuation planning under flood scenarios. Whilst the current framework operates on the basis of static flood extents, its graph-based modular structure can potentially incorporate dynamic flood data, which would enable its applicability to be extended to provide operational support for evacuation during the course of an event.

1. Introduction

Natural disasters continue to pose a direct threat to life, especially in the first few hours after the event, when decisions must be made based on incomplete information about the situation on the ground (Voigt et al., 2016). Globally, floods account for a significant proportion of weather-related disasters, and between 1998 and 2017 they affected more than 2 billion people worldwide (Douben, 2006; UNDRR, 2025; World Health Organization, 2026). In this context, the disaster that struck Central Europe in July 2021, claiming more than 200 lives, highlighted a critical shortcoming in urban resilience: the gap between the technical capacity to anticipate the event and the ability to translate that information into an effective evacuation response (Mohr et al., 2023; Tradowsky et al., 2023; Li et al., 2025).

The central problem lies in the fact that, despite advances in hydrological modelling, there is a critical gap in risk communication: the available information is not directly actionable for real-time decision-making by citizens (Kreibich et al., 2017; Apel et al., 2022; Li et al., 2025). In practice, flood warnings reach the public through a mix of channels, including official warning apps (e.g., NINA[1], KatWarn[2], Meine Pegel[3]), cell-broadcast and siren systems, as well as updates tied to river-gauge monitoring. However, receiving an alert does not necessarily mean knowing what to do next. Operational products tend to report flow rates or water levels at monitoring points, whereas traditional flood maps do not clearly show either the specific impact on buildings or the practical feasibility of movement under flood conditions (Meyer et al., 2012; Apel et al., 2022; Macchione et al., 2019). As a result, even accurate weather forecasts may not tell the public which areas remain accessible or which routes are safe to reach them (Kreibich et al., 2017; Apel et al., 2022; Tradowsky et al., 2023).

Whilst the calculation of the shortest routes on flood-restricted networks is a technique that has been explored, the contribution of this study lies not solely in calculating evacuation routes under flood conditions, but in proposing a graph-based representation that integrates, within a single spatial framework, the extent of the flooding and diverse semantic information from city models, such as buildings, the road network and the connections between them. On this basis, information on exposure and accessibility can be explicitly incorporated into the analysis, making it possible to identify not only which elements are affected, but also which connections remain viable for safe evacuation. In this way, this work moves from a static representation of the hazard towards an approach focused on effective accessibility under flood conditions.

Figure 1 illustrates the spatial outcome of the proposed approach by comparing the shortest path computed without flood constraints with the flood-aware route derived from the proposed framework. In addition to the flood extent, the figure highlights the spatial distribution of building exposure classes and illustrates how inundation alters route feasibility within the analysed area. This comparison demonstrates that the model is able to identify a safe connection between an exposed building and a destination classified as *safe*, while avoiding segments rendered inaccessible under the considered flood scenario.

To address this problem, we propose a graph-based representation of the urban environment built from open geodata, namely OpenStreetMap (OSM) and Copernicus flood extent data, and applied to the case study of Kremmen and Oranienburg, Germany. Buildings and the road network are integrated into a single connectivity system, in which the flood mask identifies and restricts affected segments to calculate the shortest safe route to an unaffected building.

[1] `https://www.bbk.bund.de/DE/Home/home_node.html`
[2] `https://www.katwarn.de/`
[3] `https://www.hochwasserzentralen.info/meinepegel/`

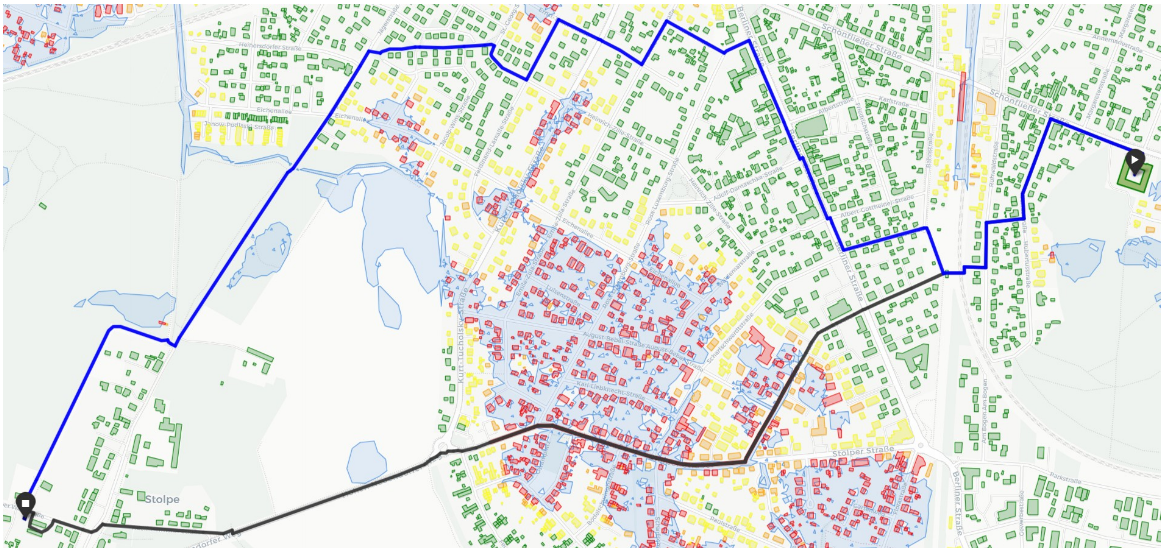

Figure 1. Comparison of routing results with and without flood constraints. The blue path represents the flood-aware route, whereas the dark path shows the shortest path computed without considering inundation. Buildings are coloured by flood-exposure class: *safe* (green), *at_risk* (yellow), *close_to* (orange), and *flooded* (red). Flood extent is shown in light blue.

The study thus provides a technical basis for moving beyond the mere representation of risk towards more action-oriented products, in which flood information can be translated into specific spatial recommendations for safe evacuation (Apel et al., 2022; Mohr et al., 2023).

Even though the implementation presented is based on a static flood mask, the structure of the proposed framework potentially allows for the integration of dynamic or real-time flood data, making it a suitable basis for operational use both during and after a flood event.

2. Related Work

Research on emergency management shows that, in natural disasters of various kinds (floods, tsunamis, earthquakes), the response during the first few hours is often limited by incomplete or contradictory information and by difficulties in coordinating decisions under pressure (Zlatanova and Holweg, 2004; Voigt et al., 2016). In the case of floods, this challenge is not merely technical but also communicative: improving warning systems does not guarantee an effective public response. Studies on flood warning response in Germany show that warnings do not always lead to immediate action, while social media analysis during the 2021 European floods reveals significant public concern and predominantly negative sentiment (Kreibich et al., 2017; Li et al., 2023a).

Flood maps remain essential for risk communication and emergency planning, but do not always provide clear practical guidance for citizens (Meyer et al., 2012). 3D representations and virtual geographic environments have thus been proposed to improve the interpretability of flood impacts, making water levels easier to relate to streets and buildings for non-expert users (Macchione et al., 2019; Li et al., 2025). However, these approaches are primarily aimed at improving hazard communication and risk perception, rather than directly addressing the operational challenge of evacuation. Consequently, products aimed at the general public should provide clearer answers to three practical questions: when to evacuate, where to go and how to reach a safe place, summarised here as “2W and 1H” (Li et al., 2023b).

Another line of research focuses on urban models and explicit connectivity as a basis for emergency analysis. Early studies note that, although 3D visualisation is already available in many GIS environments, significant limitations remain for navigation and safe-route calculation due to the absence of explicit 3D structures and topologies (Zlatanova and Holweg, 2004). Composite urban models integrating 3D geometry, graphs, topology and coupled networks have since been proposed to support route calculation and network-based queries (Lee and Zlatanova, 2008).

Based on these concepts, research into evacuation routes has progressed in several directions. Some studies refine traditional 'shortest route' approaches with more realistic travel-time factors, such as gradient, pedestrian density or infrastructure characteristics (Zhu et al., 2022), while others formulate evacuation planning as a multi-objective problem involving shelter allocation and route robustness (Coutinho-Rodrigues et al., 2012). Comprehensive approaches combine hydrodynamic simulation and optimisation to support evacuation and relocation decisions under capacity and congestion constraints (Yang et al., 2025), while dynamic routing methods show that flood-induced connectivity changes require continuous re-planning to reduce entrapment risk (He et al., 2021). Interactive flood evacuation tools have also been proposed, combining building-risk detection, safe-route identification, shelter selection, and shortest-route calculation based on time-series simulations of the floodwater's advance (Li et al., 2023b). However, there is still scope for approaches that integrate, within a single graph structure, the layout of buildings, their access links to the road network, and connectivity restricted by flooding, in order to calculate operationally safe evacuation routes.

3. Methodology

As shown in Figure 2, the proposed workflow integrates three main sources of spatial information: the flood extent, building footprints, and the road network. These layers are first cropped to a common study area and reprojected into a shared spatial reference system, so that flooding, buildings, and roads can be analysed consistently within the same domain. On this basis, buildings are connected to the road network and incorporated into a single graph that supports the subsequent flood-constrained routing analysis. At the same time, the flood layer is used both to characterise the level of building exposure and to restrict network passability. This distinguishes destinations that are merely close from those that are actually accessible under flood conditions. Finally, safe routes are calculated on the restricted graph and reconstructed as route geometries for mapping and visual inspection.

3.1 Data sources and spatial pre-processing

The analysis draws on three complementary spatial sources: flood extent, building footprints, and the road network. Flood information is obtained from the Copernicus EMSN068 product for Brandenburg [4], Germany, while buildings and the road network are extracted from OpenStreetMap via Geofabrik. The flood extent defines a common study area, to which the other layers are cropped, with a small margin added to the road network to preserve connectivity at the domain's edges. All data are harmonised in a shared spatial reference system (mainly EPSG:25832), enabling consistent computation of distances, buffers, and spatial intersections in the subsequent classification and graph-construction stages.

3.2 Graph-based evacuation model under flood constraints

Once the spatial preprocessing stage is completed, an integrated representation of the urban environment is defined in the form of a graph, with the aim of jointly modelling buildings and road infrastructure within a single analytical framework. In this formulation, the road network is represented as a graph

$$R = (V_R, E_R),$$

where V_R denotes the set of road nodes and $E_R \subseteq V_R \times V_R$ the set of edges corresponding to road segments. Each edge $e \in E_R$ is associated with a weight $w(e) \in \mathbb{R}^+$ representing the length of the corresponding road segment.

Meanwhile, the set of buildings is defined as

$$B = \{b_1, b_2, \ldots, b_m\},$$

where each building $b \in B$ is associated with a centroid position $x(b) \in \mathbb{R}^2$ and a footprint geometry $\mathrm{geom}(b)$. This distinction preserves the building's polygonal geometry for subsequent spatial analyses, while also defining a reference point for its integration into the connectivity model.

To integrate both components, each building $b \in B$ is connected to its nearest road node through a projection operator

$$\pi : B \to V_R,$$

defined as

$$\pi(b) = \arg\min_{v \in V_R} \|x(b) - x(v)\|.$$

[4] https://mapping.emergency.copernicus.eu/activations/EMSN068/

Thus, each building is linked to the road network node that minimises its spatial distance, allowing for its effective inclusion in the accessibility analysis.

Based on these relationships, the integrated graph is constructed

$$G = (V, E),$$

with

$$V = V_R \cup B,$$

and

$$E = E_R \cup E_B,$$

where

$$E_B = \{(b, \pi(b)) \mid b \in B\},$$

represents the set of access routes between each building and its nearest network node. The weight of each of these connections is defined as

$$w(b, \pi(b)) = \|x(b) - x(\pi(b))\|,$$

so that the connection between the building and the road network is also included in the total travel cost.

This represents, within a single structure, both road network connectivity and the buildings' initial accessibility. The integrated graph thus serves as the analytical foundation for incorporating, in subsequent stages, both flood vulnerability and network mobility restrictions.

3.2.1 Semantic building–flood relations

Once the integrated graph has been constructed, the flood geometry is used to characterise the degree of exposure of each building. To this end, a semantic relation between buildings and the flood extent $F \subset \mathbb{R}^2$ is defined as

$$\texttt{exposed\_to} \subseteq B \times F,$$

such that

$$(b, F) \in \texttt{exposed\_to} \iff \mathrm{geom}(b) \cap F \neq \emptyset.$$

This relationship makes it possible to identify the buildings directly affected by the flooding and, on that basis, to establish a hierarchical classification of exposure based on the geographical proximity between each building and the flooded area.

Based on this relation, buildings are classified into four categories:

- *flooded*: $\mathrm{geom}(b) \cap F \neq \emptyset$,
- *close_to*: $d(\mathrm{geom}(b), F) \leq \varepsilon_1$,
- *at_risk*: $\varepsilon_1 < d(\mathrm{geom}(b), F) \leq \varepsilon_2$,
- *safe*: otherwise,

where $d(\cdot, \cdot)$ denotes the minimum distance between geometries and $\varepsilon_1 < \varepsilon_2$ are distance thresholds.

In this study, these thresholds are defined using two buffer zones generated from the flood layer, with $\varepsilon_1 = 10$ m for the *close_to* category and $\varepsilon_2 = 50$ m for the *at_risk* category. This allows

https://doi.org/10.5194/isprs-annals-XII-4-W2-2026-195-2026 | © Author(s) 2026. CC BY 4.0 License.

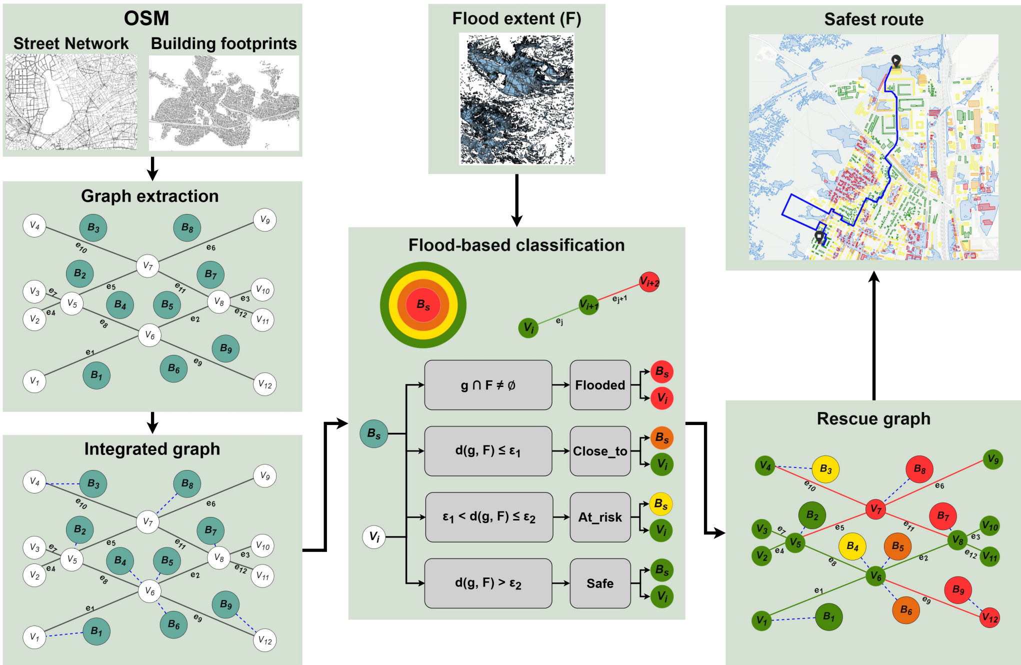

Figure 2. Workflow of the proposed methodology for integrating flood extent (F) into a graph-based safe-routing model. A graph is extracted from OSM street network and building footprint data and integrated into a unified spatial representation. Flood information is incorporated by classifying geometries g according to their flood exposure and by assigning a prohibitively large cost to flooded road segments, thereby yielding a flood-constrained rescue graph for safe route derivation.

the classification to incorporate not only buildings directly affected by flooding, but also a spatial gradation of exposure in the surrounding area. To ensure mutually exclusive classes, the categories are assigned sequentially.

The resulting exposure status is incorporated as a semantic attribute into each building node, alongside its geometry and building type. This label supports both the spatial interpretation of the scenario and the selection of origins and destinations in the subsequent analysis of safe routes.

3.2.2 Flood-constrained graph

After defining the integrated graph and assigning exposure status to buildings, the flood layer is also used to identify the affected road segments and to incorporate their impact into the routing model. To this end, the spatial interaction between each road-segment geometry and the flood extent is evaluated, so that segments intersecting the flooded area can be represented as operationally unavailable under the analysed scenario. On this basis, a modified cost function w' is defined, which incorporates the constraints imposed by flooding on the street network. For road links, this function can be expressed as

$$w'(e) = \begin{cases} \infty & \text{if } e \cap F \neq \emptyset, \\ w(e) & \text{otherwise.} \end{cases}$$

where $w(e)$ corresponds to the original cost of the edge, defined in terms of its geodetic length. Consequently, the flooded segments acquire a prohibitively large cost and are excluded from the routing process, while the unaffected segments retain a finite cost corresponding to their length.

In the case of access routes between buildings and the road network, the cost remains linked to their length, so that these connections continue to form part of the total cost of travel.

This yields a flood-constrained weighted graph:

$$G' = (V, E, w'),$$

in which the original connectivity structure is retained, but its usage is modified by the new cost function. From this graph, the set of operational edges can be defined as

$$E_f = \{e \in E \mid w'(e) < \infty\}$$

and, consequently, the graph representing flood-conditional connectivity as

$$G'_f = (V, E_f).$$

This restricted graph distinguishes geometric connectivity from actual accessibility: spatial proximity between two buildings does not imply a safe route between them, since this depends on the continuity of unaffected road segments in the residual network. In this sense, flooding is incorporated not merely as a descriptive element of the environment but as a spatial constraint that explicitly alters the passability of the urban system.

Furthermore, by applying the restriction at the segment level rather than at the level of the entire street, the model preserves those sub-sections that remain dry and connected, thereby avoiding unnecessary blockages and maintaining the greatest possible continuity of the network. On this basis, the subsequent stages of selecting reachable destinations and calculating safe routes are carried out exclusively on the resulting operational graph G'_f.

3.2.3 Accessible buildings and routing

Having constructed the flood-restricted graph, the next step is to identify which buildings can be effectively reached from a given origin and, from among these, to select those that are suitable as evacuation destinations. Let $b_s \in B$ be an origin building. The set of buildings reachable from b_s is defined as

$$\mathcal{R}(b_s) = \{b \in B \mid \exists \text{ path } P \text{ in } G'_f \text{ from } b_s \text{ to } b\}.$$

A building may thus be geometrically close to the origin yet remain inaccessible if flooding has interrupted the continuity of passable segments.

Based on this set, the permissible destinations are restricted to those buildings previously classified as *safe*, so that

$$\mathcal{D}(b_s) = \mathcal{R}(b_s) \cap B_{\text{safe}},$$

where

$$B_{\text{safe}} = \{b \in B \mid \text{geom}(b) \cap F = \emptyset\}.$$

Consequently, a potential destination must not only be accessible within the operational network, but must also be located in an area deemed safe under the flood scenario analysed.

After defining a destination building $b_t \in D(b_s)$, the evacuation route is formulated as an optimisation problem on the restricted rescue graph. Specifically, the path P of minimum cost between the origin and the destination is sought, in accordance with the modified cost function w':

$$\min_P \sum_{i=0}^{k-1} w'(v_i, v_{i+1}),$$

subject to

$$P = (v_0, v_1, \ldots, v_k), \quad v_0 = b_s, \quad v_k = b_t,$$
$$(v_i, v_{i+1}) \in E, \quad w'(v_i, v_{i+1}) < \infty.$$

The optimisation is solved using the A* algorithm, where each node $n \in V$ is evaluated according to

$$f(n) = g(n) + h(n),$$

with $g(n)$ denoting the accumulated cost from the origin and $h(n)$ a heuristic estimate of the remaining distance to the destination.

The proposed formulation integrates semantic information on building exposure with topological constraints on the road network. This allows a clear distinction between geometric proximity and effective accessibility, ensuring that evacuation routes are computed only through operationally available paths. The resulting workflow not only identifies exposed buildings but also reveals how flooding alters urban connectivity and constrains feasible movement within the study area.

3.3 Route reconstruction and cartographic visualisation

Once the safe route between the source building and the destination building has been obtained, it is reconstructed at the segment level to facilitate spatial interpretation. For this purpose, the edges that make up the final trajectory are recovered and two types of connection are distinguished: the actual segments of the road network and the access edges that link each building to its nearest network node. While the road sections retain their original geometry, the access connections are represented by straight lines between the centroid of the building and the corresponding road node.

Based on this reconstruction, each segment of the route is described using attributes such as sequential order, length, type of relationship, and flood-related status. In the case of road sections, when information is available, descriptive attributes from OpenStreetMap are also incorporated, such as street name, reference, or road type. This procedure makes it possible to transform the output of the routing algorithm into an interpretable sequence of steps, facilitating both the verification of the result and the detailed interpretation of the resulting route.

For cartographic representation, the geometries of the route and selected buildings are reprojected to EPSG:4326 for web-based visualisation and subsequently integrated into an interactive map. In this visualisation, the origin and destination buildings are represented differently, while road segments and building-network connections are symbolised with different styles to make the structure of the trajectory explicit. In order to improve the clarity of the result, the floodplain layer is not displayed in its entirety, but is dynamically cropped using a buffer generated around the route. In this way, the map focuses attention on the spatial corridor relevant to the journey under analysis and avoids unnecessary visual clutter.

The final visualisation serves a dual purpose: it validates that the calculated route fits the available network, avoids flooded segments, and aligns visually with building exposure classes and excluded road sections; and it provides a clear analytical output for communicating how flooding conditions movement within the urban environment.

The resulting route therefore corresponds to the shortest safe route within the flood-restricted network, where safety is defined by the exclusion of flooded road segments and routing cost remains proportional to segment length. For each calculated route, the total travelled distance is obtained as the sum of the lengths of the segments used, and it is verified that the final itinerary does not include flooded road sections. In this way, the procedure enables the calculation of safe routes between selected buildings and the assessment of how flooding affects local accessibility within the study area.

4. Results

4.1 Overview of computed safe routes under flood constraints

To evaluate the performance of the proposed routing model, five representative origin-destination building pairs were selected, based on the prior classification of exposure and accessibility. In each case, the route was calculated on the flood-restricted network, excluding segments that intersected the floodplain. The selection included four long routes, useful for clearly demonstrating the spatial detours induced by flooding, and an additional short-distance case, included as a comparative reference. In all five cases analysed, the algorithm identified a complete connection between the starting building and a building classified as safe, without using any flooded road segments. Taking the entire set of cases into account, the distances obtained ranged from $410.6\,\text{m}$ to $3997.4\,\text{m}$. However, as one of the cases was included as a short-distance benchmark, the four long routes are described separately: their lengths ranged from $3598.7\,\text{m}$ to $3997.4\,\text{m}$, with an average of $3825.1\,\text{m}$, while the short comparative case was only $410.6\,\text{m}$. Furthermore, in all cases, two access edges were maintained and no flooded sections were used.

https://doi.org/10.5194/isprs-annals-XII-4-W2-2026-195-2026 | © Author(s) 2026. CC BY 4.0 License.

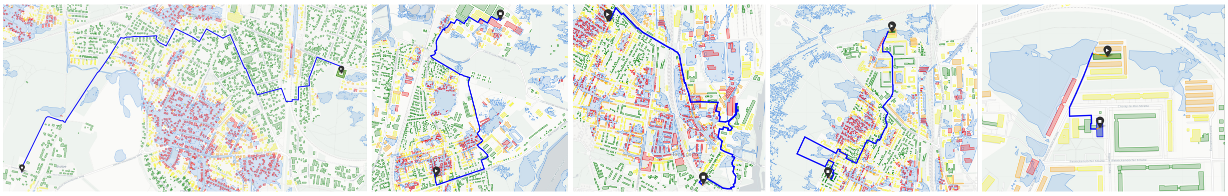

(a) Case 1 (b) Case 2 (c) Case 3 (d) Case 4 (e) Case 5

Figure 3. Five representative examples of safe routes calculated between buildings under the flood scenario. Cases 1–4 correspond to long routes selected for their illustrative value, whereas Case 5 provides a short-distance benchmark to the nearest safe destination. In all cases, the computed route avoids flooded road segments.

4.2 Routing patterns under flood constraints

The first four cases selected as long routes (Cases 1–4 in Figure 3) demonstrate how flooding alters the network's accessibility and forces the algorithm to construct safe paths with different spatial configurations. Although all routes fall within a similar length range, between $3598.7\,\mathrm{m}$ and $3997.4\,\mathrm{m}$, the model's response does not follow a single geometric pattern.

In summary, the effect of flooding on route selection cannot be described solely in terms of additional distance: hydrological constraints also reshape the route's geometry, taking the form of a wide detour around a compromised sector, a more fragmented sequence of local connections, or a shift towards lateral or peripheral corridors. The long routes obtained should therefore not be interpreted as uniform algorithmic behaviour, but as a response spatially conditioned by the location of safe destinations and the connectivity available in the non-flooded network.

This interpretation is supported by comparing two routes from the same origin, **A**, to safe destinations at different distances. In Case 4, the route connects **A** to a more distant safe destination, **B**, over $3598.7\,\mathrm{m}$. In Case 5, the same origin is linked to the nearest reachable safe building, **C**, over just $410.6\,\mathrm{m}$. This comparison shows that the long routes observed are not an artificial effect of the model, but a direct consequence of the spatial structure of safe accessibility under flood conditions: routes remain short when a nearby safe destination is connected via non-flooded segments, and must extend otherwise. Figure 4 illustrates this contrast.

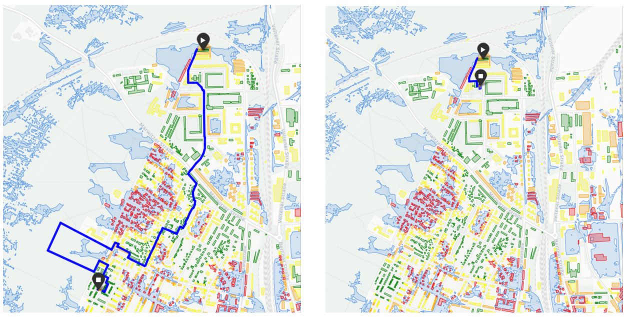

(a) Case 4 (b) Case 5

Figure 4. Comparison of two safe routes from the same origin building. Case 4 shows a longer route to a more distant safe destination, whereas Case 5 shows a shorter route to the nearest safe destination. In both sub-figures, the route avoids flooded road segments.

4.3 Segment-level flood blocking and local route rejoining

A particularly noteworthy aspect of the proposed model is illustrated in Case 5, where the impact of flooding on road connectivity can be examined at a local scale. Rather than treating streets as indivisible entities, the model represents the road network as graph edges corresponding to individual segments between consecutive nodes, so the flood restriction applies only to segments intersecting the flooded area, not entire streets.

This segment-level treatment avoids unnecessary street-level exclusion: instead of discarding an entire street whenever one part is flooded, the algorithm excludes only the affected edge, preserving dry segments that remain topologically connected. Local route rejoining is thus possible when dry subsegments remain reachable through adjacent nodes or alternative connections; where such connectivity is unavailable, however, a single flooded segment may still block movement along the corridor, providing a more precise representation of how flooding affects the network's effective connectivity.

Figure 5 shows, at a local scale, an example in which the model handles a partial disruption of road connectivity under flood conditions. In this case, only the segment that crosses the flooded area is excluded from routing, while subsequent dry subsegments remain available and can be reused by the route. This example illustrates the technical value of the proposed approach, showing that routing not only avoids flooded sections but can also preserve local connectivity where dry, connected segments still exist. In this sense, the model does not indiscriminately generate wide detours, but adjusts the route at the level of the segmented road network whenever the residual topology allows it.

5. Discussion

5.1 Strengths of the graph-based representation

One of the main contributions of this study is a graph-based representation that integrates buildings, road segments, and their access relationships into a single analytical framework, in which the flood mask acts as a spatial constraint identifying affected sections and determining network passability. This allows the built environment to be modelled not as a collection of isolated geographic objects, but as a functional network in which each building is explicitly linked to the available mobility infrastructure under threat conditions. Accessibility is thus assessed by which connections are effectively passable, not by geometric proximity alone.

In addition to representing connectivity under hazardous conditions, the proposed graph offers a flexible framework for future research: its structure allows new attributes for buildings,

This contribution has been peer-reviewed. The double-blind peer-review was conducted on the basis of the full paper.
https://doi.org/10.5194/isprs-annals-XII-4-W2-2026-195-2026 | © Author(s) 2026. CC BY 4.0 License.

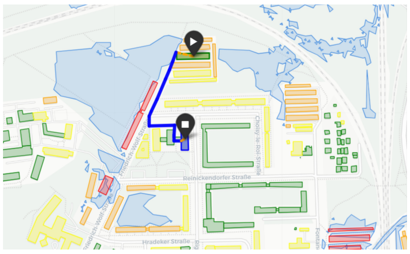

(a)

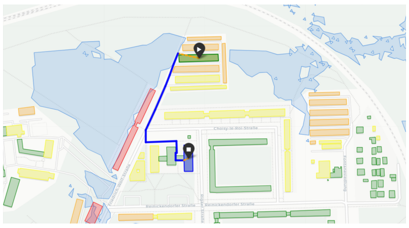

(b)

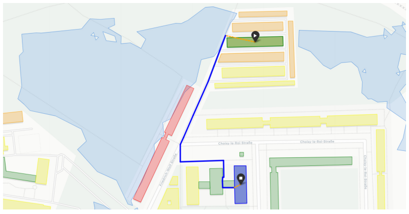

(c)

Figure 5. Local-scale example of route behaviour in Case 5. Sub-figures (a)–(c) show progressively closer views of the affected area. The flooded segment is excluded from routing, while the remaining dry segments preserve route connectivity.

nodes, or road segments to be incorporated without redefining the analytical framework, facilitating additional datasets and new routing criteria. This would also make it possible to calculate routes to specific functional destinations, such as schools, hospitals, or shelters, provided such information is encoded in the graph. The same problem can be addressed without an explicit graph structure: cellular automata approaches (He et al., 2021) capture the dynamic evolution of flooding but without semantic integration of buildings, whereas raster-based approaches (Petricola et al., 2022) do not depend on road-network completeness, though they sacrifice spatial resolution where the network is well mapped, as in the study area considered here. The approach is thus useful not only for calculating safe routes here, but as a methodological foundation for more complex analyses of accessibility, exposure, and evacuation in flood contexts.

5.2 Directions for further development

Beyond the results obtained, the proposed model is best understood as a flexible, modular, graph-based framework for evacuation routing in flood scenarios, capable of incorporating additional variables, such as priority routing for emergency services, and refining its routing logic in future work, although this potential was not exploited in the experiments presented here.

One of the most significant extensions involves incorporating additional information on the physical severity of the flooding, such as water depth or relative ground elevation. In the current formulation, segment passability is binary: a section affected by flooding is either permissible or not, and therefore

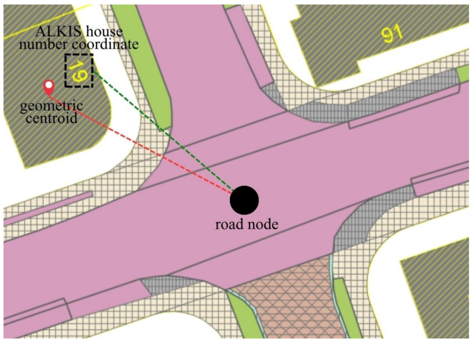

Figure 6. Geometric centroid versus ALKIS house number coordinate as reference points for connecting a building to the road network, yielding a more realistic access edge to the nearest road node. *Source: Geoportal Hamburg (ALKIS viewer).*

excluded from the analysis. A more detailed representation would instead allow gradual penalties based on impact intensity. For example, a segment with low estimated water depth could still be considered navigable at a lower speed, whereas greater depths would exclude it entirely. This depth information could also yield a route-level quantitative metric, such as cumulative or maximum water exposure along the route, complementing length as an evaluation criterion.

Given its reliance on a static flood mask, a route calculated as safe could be compromised if the flooding continues to advance during the evacuation, and the travel mode (pedestrian or vehicular) is not specified in the current formulation, although it directly affects the actual feasibility of a route. Similarly, the values of ε_1 and ε_2 used in this study do not derive from a universal standard established in the scientific literature, and can be adjusted according to the local context, including, where applicable, water-safety regulations in force in the corresponding jurisdiction. In this sense, the developed model should not be understood as a final result, but rather as an initial platform upon which to build more realistic, context-sensitive analyses open to the integration of new datasets.

In Germany's Authoritative Cadastral Information System (ALKIS)[5](German: *Amtliches Liegenschaftskatasterinformationssystem*) the house number of a building is assigned the exact coordinate of its main entrance. As a possible improvement, each building's centroid could be replaced by the coordinate of the building's house number, as shown in Figure 6, thus offering a more representative reference of actual access.

6. Conclusions & Outlook

This study presented a graph-based safe-routing approach that integrates buildings, the road network, and the flood mask as a spatial constraint on traversability, to identify safe routes connecting exposed buildings with destinations classified as safe. In all cases analysed, the model avoided flooded road segments and produced paths consistent with the connectivity actually available. The main contribution of this work thus lies in the integrated graph-based formulation itself, linking buildings and mobility infrastructure to support flood-constrained routing and accessibility analysis.

Beyond the static scenario considered here, several directions for further development emerge. First, the current formulation

[5] `https://www.berlin.de/sen/sbw/stadtdaten/geoportal/liegenschaftskataster/alkis/`

could be extended towards more proactive routing, in which routes are selected not only by avoiding flooded segments, but also by maintaining a safety buffer from inundated areas in order to account for possible flood expansion during evacuation. Second, future work should move beyond static flood information and incorporate dynamic or real-time flood updates. In this context, the graph-based structure proposed in this study offers a suitable basis for efficiently updating building accessibility and road passability as conditions evolve. More generally, the framework can be extended with additional variables, such as water depth, terrain elevation, or other context-sensitive routing factors, to support more realistic and customisable evacuation analyses in flood scenarios.

7. Acknowledgement

This research was supported by the project "Next Generation City Networking" (Grant No. 19DZ24004) at the Hanseatic Wireless Innovation Competence Center (HAWICC). The project is funded by the Federal Ministry of Transport via the German Center for Future Mobility (DZM).

References

Apel, H., Vorogushyn, S., Merz, B., 2022. Brief communication: impact forecasting could substantially improve the emergency management of deadly floods: case study July 2021 floods in Germany. *Natural Hazards and Earth System Sciences*, 22, 3005–3014.

Coutinho-Rodrigues, J., Tralhão, L., Alçada-Almeida, L., 2012. Solving a location-routing problem with a multiobjective approach: the design of urban evacuation plans. *Journal of Transport Geography*, 22, 206–218.

Douben, K.-J., 2006. Characteristics of river floods and flooding: a global overview, 1985–2003. *Irrigation and Drainage*, 55(S1), S9–S21.

He, M., Chen, C., Zheng, F., Chen, Q., Zhang, J., Yan, H., Lin, Y., 2021. An efficient dynamic route optimization for urban flooding evacuation based on cellular automata. *Computers, Environment and Urban Systems*, 87, 101622.

Kreibich, H., Müller, M., Schröter, K., Thieken, A. H., 2017. New insights into flood warning reception and emergency response by affected parties. *Natural Hazards and Earth System Sciences*, 17, 2075–2092.

Lee, J., Zlatanova, S., 2008. A 3D data model and topological analyses for emergency response in urban areas. S. Zlatanova, J. Li (eds), *Geospatial Information Technology for Emergency Response*, Taylor & Francis, Leiden, 143–168.

Li, W., Haunert, J.-H., Knechtel, J., Zhu, J., Zhu, Q., Dehbi, Y., 2023a. Social media insights on public perception and sentiment during and after disasters: the European floods in 2021 as a case study. *Transactions in GIS*, 27, 1766–1793.

Li, W. L., Treff, N., Amann, F., Lehmen, J., Dehbi, Y., Haunert, J.-H., 2023b. An interactive evacuation tool to improve the public flood perception. *ISPRS Geospatial Week 2023*, The International Archives of the Photogrammetry, Remote Sensing and Spatial Information Sciences, XLVIII-1/W2-2023, Cairo, Egypt, 437–440.

Li, W., Zhu, J., Pirasteh, S., Zhu, Q., Guo, Y., Luo, L., Dehbi, Y., 2025. A 3D virtual geographic environment for flood representation towards risk communication. arXiv:2512.03839v1.

Macchione, F., Costabile, P., Costanzo, C., De Santis, R., 2019. Moving to 3-D flood hazard maps for enhancing risk communication. *Environmental Modelling & Software*, 111, 510–522.

Meyer, V., Kuhlicke, C., Luther, J., Fuchs, S., Priest, S., Dorner, W., Serrhini, K., Pardoe, J., McCarthy, S., Seidel, J., Palka, G., Unnerstall, H., Viavattene, C., Scheuer, S., 2012. Recommendations for the user-specific enhancement of flood maps. *Natural Hazards and Earth System Sciences*, 12, 1701–1716.

Mohr, S., Ehret, U., Kunz, M., Ludwig, P., Caldas-Alvarez, A., Daniell, J. E., Ehmele, F., Feldmann, H., Franca, M. J., Gattke, C., Hundhausen, M., Knippertz, P., Küpfer, K., Mühr, B., Pinto, J. G., Quinting, J., Schäfer, A. M., Scheibel, M., Seidel, F., Wisotzky, C., 2023. A multi-disciplinary analysis of the exceptional flood event of July 2021 in central Europe – Part 1: event description and analysis. *Natural Hazards and Earth System Sciences*, 23, 525–551.

Petricola, S., Reinmuth, M., Lautenbach, S., Hatfield, C., Zipf, A., 2022. Assessing road criticality and loss of healthcare accessibility during floods: the case of Cyclone Idai, Mozambique 2019. *International Journal of Health Geographics*, 21, 14.

Tradowsky, J. S., Philip, S. Y., Kreienkamp, F., Kew, S. F., Lorenz, P. et al., 2023. Attribution of the heavy rainfall events leading to severe flooding in Western Europe during July 2021. *Climatic Change*, 176(90).

UNDRR, 2025. GAR 2025 hazard explorations: floods. `https://www.undrr.org/gar/gar2025/hazard-exploration/floods`. Accessed: 2026-02-23.

Voigt, S., Giulio-Tonolo, F., Lyons, J., Kučera, J., Jones, B., Schneiderhan, T., Platzeck, G., Kaku, K., Hazarika, M. K., Czaran, L., Li, S., Pedersen, W., James, G. K., Proy, C., Muthike, D. M., Bequignon, J., Guha-Sapir, D., 2016. Global trends in satellite-based emergency mapping. *Science*, 353(6296), 247–252.

World Health Organization, 2026. Floods. `https://www.who.int/health-topics/floods`. Accessed: 2026-02-23.

Yang, W., Yan, X., Hu, D., Jiang, X., Song, J., Lang, R., Xu, K., Lian, J., 2025. A novel emergency evacuation route optimization model in flood disasters using hydrodynamic model and intelligent algorithm. *Safety Science*, 182, 106709.

Zhu, Y., Li, H., Wang, Z., Li, Q., Dou, Z., Xie, W., Zhang, Z., Wang, R., Nie, W., 2022. Optimal evacuation route planning of urban personnel at different risk levels of flood disasters based on the improved 3D Dijkstra's algorithm. *Sustainability*, 14(16), 10250.

Zlatanova, S., Holweg, D., 2004. 3D geo-information in emergency response: a framework. *Proceedings of the 4th International Symposium on Mobile Mapping Technology (MMT 2004)*, Kunming, China. 6 p.